Fan, H., Bolhuis, H. & Stal, L. (2015). Denitrification and the denitrifier community in coastal microbial mats. *FEMS Microbiology Ecology*, 91(3), 11 pp.

Published version: dx.doi.org/10.1093/femsec/fiu033
Link NIOZ Repository: www.vliz.be/nl/imis?module=ref&refid=246525

DENITRIFICATION AND THE DENITRIFIER COMMUNITY IN COASTAL MICROBIAL MATS

Haoxin Fan[1], Henk Bolhuis[1], and Lucas J. Stal[1,2]

[1]Department of Marine Microbiology, Royal Netherlands Institute of Sea Research, Yerseke, The Netherlands

[2]Department of Aquatic Microbiology, Institute of Biodiversity and Ecosystem Dynamics, University of Amsterdam, The Netherlands

Running head: Denitrification in a coastal microbial mat.

Correspondence: Lucas J. Stal, Department of Marine Microbiology, Royal Netherlands Institute for Sea Research, PO Box 140, 4400 AC Yerseke, The Netherlands. Tel.: +31 113 577 497; Fax: +31 113 573 616

E-mail: Lucas.Stal@nioz.nl

Keywords**:** Denitrification, microbial mat, *nirK*, *nirS*

Abstract

Denitrification was measured in three structurally different coastal microbial mats by using the stable isotope technique. The composition of the denitrifying community was determined by analyzing the nitrite reductase (*nirS* and *nirK*) genes using clone libraries and the GeoChip. The highest potential rate of denitrification (7.0±1.0 mmol N m^{-2} d^{-1}) was observed during summer at station 1 (supra-littoral). The rates of denitrification were much lower in the stations 2 (marine) and 3 (intermediate) (respectively 0.1 ±0.05 and 0.7±0.2 mmol N m^{-2} d^{-1}) and showed less seasonality when compared to station 1. The denitrifying community at station 1 was also more diverse than that at station 2 and 3, which were more similar to each other than either of these stations to station 1. In all three stations, the diversity of both *nirS*- and *nirK*-denitrifiers was higher in summer when compared to winter. The location along the tidal gradient seems to determine the composition, diversity and activity of the denitrifier community, which may be driven by salinity, nitrate/nitrite and organic carbon. Both *nirS* and *nirK* denitrifiers are equally present and therefore they are likely to play a role in the denitrification of the microbial mats studied.

Introduction

Denitrification is a bacterial process during which nitrate or nitrite is stepwise reduced through a few intermediate gaseous nitrogen compounds to dinitrogen (Zumft, 1997). Nitrite reductase is present in all denitrifying bacteria and mediates the reduction of nitrite to nitric oxide and is considered as the key enzyme of denitrification. There are two functional equivalent but structurally distinct nitrite reductases known in denitrifying bacteria (Zumft, 1997). These are Cytochrome cd1 (Cd-Nir), encoded by *nirS* and a copper nitrite reductase (Cu-Nir), encoded by *nirK*. There are no organisms known that carry both genes and therefore these two enzymes are thought to be mutually exclusive (Zumft, 1997). Nitrite reductase genes have been used as functional molecular markers for denitrification in natural environments and have revealed the diversity of denitrifying bacteria in a variety of habitats such as soil (Prieme *et al.*, 2002; Throbäck *et al.*, 2007), estuarine sediments (Santoro *et al.*, 2006), marine sediments (Braker *et al.*, 2000; Hannig *et al.*, 2006), and seawater (Castro-Gonzalez *et al.*, 2005; Jayakumar *et al.*, 2004; Oakley *et al.*, 2007). Environmental factors were identified that shaped the denitrifier community composition (Braker *et al.*, 2000; Hallin *et al.*, 2009). Moreover, the type of habitat determined the presence or dominance of *nirS*- and *nirK*- type denitrifiers (Hannig *et al.*, 2006; Oakley *et al.*, 2007).

Coastal microbial mats are compact, highly structured, small-scale ecosystems (Stal, 2001). These mats are built by cyanobacteria, oxygenic phototrophic bacteria, which through primary production enrich the sediment with organic matter. This organic matter forms the basis of a complex, multi-layered microbial ecosystem. Previous studies of nitrogen cycling in microbial mats have focused mainly on the nitrogen fixation and only a few studies documented denitrification in microbial mats. Joye & Paerl (1994) studied denitrification in microbial mats of Tomales Bay (California) and found that it removed only 15% of the N_2 that was fixed on an annual basis in these mats. In a hypersaline microbial mat, denitrification was lower than N_2 fixation in summer, but exceeded N_2 fixation in winter when it turned the mat into a sink for nitrogen (Bonin & Michotey, 2006). Desnues *et al.* (2007) reported spatio-temporal distribution of denitrifying bacteria in a hypersaline microbial mat. These studies focused on the rates of denitrification and did not give information on the diversity and the temporal and spatial distribution of the denitrifying bacteria and their activities and therefore provided only an incomplete view on this process in microbial mats.

We investigated microbial mats that proliferate at the North Sea coast of the Dutch barrier island Schiermonnikoog. Based on morphological, microscopic, and molecular genetic differences we distinguish three major types of microbial mats that develop along the tidal gradient. The bacterial, archaeal and eukaryal community composition and microbial diversity were intrinsic of the mat type and depended on the location along the tidal salinity gradient (Bolhuis & Stal, 2011; Bolhuis *et al.*, 2013). Previously it was shown that N_2 fixation and the diazotrophic community varied along the same lines at these three stations (Severin & Stal, 2010). The variation of N_2 fixation may be attributed to different environmental conditions in microbial mats, which changes spatially (location along the tidal gradient) and temporally (tide, day-night, and seasonal). We expect that the same factors exert also a selective force on the denitrifying community and its activity. At the different positions along the tidal gradient the mats would allow the development of different community compositions, which would also alter the potential rate of denitrification that can be achieved (Philippot & Hallin, 2005). In this study we measured the potential rates of denitrification in the three different mat types during different seasons. Alongside, we identified the denitrifying communities and measured relevant environmental variables in order to elucidate: 1) whether mats along the tidal gradient contain different types of denitrifying bacteria; 2) whether a relationship exists between the denitrifier community and the potential rate of denitrification; 3) which environmental factors affect denitrification and the composition of the denitrifier communities.

Material and methods

Study area and sampling

The study site was located on the North Sea coast of the Dutch barrier island Schiermonnikoog. The geographical locations and descriptions of the three types of microbial mats (stations) that were sampled for this study are given in Table 1. The sample stations were situated along a transect perpendicular to the beach covering the tidal gradient. Sampling was done at four different seasons during 2010 and 2011. Samples were taken from the top 2.5-3 cm of the mat using custom-made transparent Lexan cylinder cores of 50 mm inner diameter and 60 mm height. The cores were transported back to the laboratory within 4 h of sampling and kept at ambient temperature and light. The incubations started within 24 h after sampling. Additional samples were taken for nucleic acid extraction. These samples were taken from the top 1 cm of the mat by using a 10 ml truncated syringe as a corer. These mat samples were divided into four equal parts, put into cryo-vials, and immediately frozen in the field in liquid nitrogen.

Chemical analyses

For nutrient analyses 5 g mat sample (top 1 cm) was extracted with 40 ml 2 *M* KCl. The extracts were filtered through Whatman GF/F filters and the filtrates were kept at -20 °C until analysis (within a month). Nutrient concentrations were measured on an automated Segmented Flow Analyzer using standard analytical procedures. Other mat samples were freeze-dried for the determination of total nitrogen (TN), total organic carbon (TOC) and C/N ratio by EA-IRMS (DELTA V Advantage; Thermo Fisher Scientific, Bremen, Germany).

Measurement of potential denitrification

Subsamples of 1.2 cm^2 (10 mm thickness) of the cores of the mats were placed into 12.5 ml Exetainers (Labco Limit, Buckinghamshire, England) by using a 5-ml syringe as a corer. The measurements were carried out according to Thamdrup & Dalsgaard (2002) with some modifications. Briefly, the Exetainers were completely filled with anoxic artificial seawater (NaCl 20.5 g, Na_2SO_4 3.4 g, KCl 0.58 g, KBr 0.084 g and H_3BO_3 0.022 g, $MgCl_2.6H_2O$ 0.05 mol, $CaCl_2.2H_2O$ 0.01 mol in 1000 ml Milli-Q water). Addition of 100 µM $Na^{15}NO_3$ (98.5%, ^{15}N atom%; Sigma-Aldrich, 100 µM $^{15}NH_4Cl$ (99.2%, ^{15}N atom%; Sigma-Aldrich) and 100 µM $^{15}NH_4Cl$ +100µM $Na^{14}NO_3$ were applied to the Exetainers, respectively. Before the addition of the ^{15}N tracer, the Exetainers were placed in dark for 2 h to allow the depletion of NO_x^- and any residual oxygen. All Exetainers, including one set without any addition, were incubated for 24 h in the dark at ambient temperature (Table 2). At 4-h intervals during 24 h two replicate Exetainers from each treatment were fixed by injecting 200 µl 50% (w/v) $ZnCl_2$. The Exetainers were stored at 4°C in the dark upside down until analysis (within a week). The isotopic composition of the dinitrogen of He-equilibrated headspace (2 ml in the 12.5-ml Exetainer vials) was determined by an EA-IRMS (DELTA V Advantage; Thermo Fisher Scientific, Bremen, Germany) equipped with a Haysep Q column. The potential rate of denitrification was calculated from the linear production of excess $^{29}N_2$ and $^{30}N_2$ according to Thamdrup & Dalsgaard (2002).

DNA extraction, PCR, cloning and sequencing

DNA was extracted using the MoBio UltraCLEAN soil DNA kit (MoBio Laboratories, Inc., Carlsbad, CA, USA) according to the manufacturer's instructions. Fragments of the genes *nirS* and *nirK* were amplified using the primer pairs cd3aF-R3cd for *nirS* and F1aCu-R3Cu for *nirK* (Throbäck *et al.*, 2004). PCR conditions for the two sets of primer pairs were 2 min at 95°C, 35 cycles of 50 sec 95°C, 50 sec 53°C, and 50 sec at 72°C, followed by a final extension of 10 min at 72°C. PCR products were checked on a 1% agarose gel. PCR products were cloned using the TOPO-TA cloning kit with the pcR2.1 vector and TOP10 competent cells (Invitrogen, Carlsbad, CA, USA) following the manufacturer's instructions. Transformants were randomly picked from each clone library and screened by PCR using T3 and T7 vector primers following the recommended PCR conditions (Invitrogen, Carlsbad, CA, USA). Forty-eight clones were randomly selected for sequencing with the T7 vector primer using ABI PRISM 3130 Genetic

Analyzer (Applied Biosystems, Foster City, CA, USA). The total number of sequences obtained from each clone library varied (28-70 sequences) due to the variable quality of the sequencing reads. Sequences have been submitted to NCBI (accession numbers KJ738332 - KJ739305).

Sequence analysis

Sequences were edited, aligned and translated using MEGA 5 (Molecular Evolutionary Genetics Analysis, http://www.megasoftware.net/mega5/mega.html) and manually checked. Neighbor-joining trees were produced and the reliability of the phylogenetic reconstructions was evaluated by bootstrapping (1000 replicates). The program Mothur (http://www.mothur.org/wiki/Main_Page) was used to calculate the non-parametric richness estimators and the Shannon diversity index and to determine the differences in nucleic acid sequences. Operational Taxonomic Units (OTUs) were defined by a 5% difference in nucleic acid sequence for the purpose of community analysis. Based on the OTUs from each library, sequence data were transformed into binary data (presence/absence) for community composition analysis.

GeoChip analysis

The GeoChip is a high-throughput functional gene array covering 289 functional gene families involved in the biogeochemical cycling of carbon, nitrogen, phosphorus and sulfur (He *et al.*, 2010). For the analysis using the GeoChip we used DNA extracted in triplicate from the three types of microbial mats sampled in July and in November. The DNA was purified using UltraClean 15 DNA purification Kit (MoBio Laboratories, Inc., Carlsbad, CA, USA) in order to achieve the quality necessary for hybridization on the chip. The DNA quantity was measured by an ND-1000 spectrophotometer (Nanodrop Inc., Wilmington, DE). The procedures for DNA labeling and microarray hybridization followed the previously established protocols (Wu *et al.*, 2006). Briefly, 800 ng of environmental DNA was labeled with fluorescent dye Cy-5 by random priming. The labeled DNA was re-suspended in 50 μl hybridization solution [40% formamide, 5 x SSC, 5 μg of unlabeled herring sperm DNA (Promega, Madison, WI), and 0.1% SDS] and 2 μl universal standard DNA (0.2 pmol μl^{-1}) labeled with the fluorescent dye Cy-3 (Liang *et al.*, 2010), denatured at 95°C for 5 min and maintained at 50°C until loaded onto the microarray slides. Arrays were hybridized on a MAUI Hybridization Station (Roche, South San Francisco, CA) for 12 h at 42ºC. Hybridized microarrays were scanned by a ScanArray Express Microarray scanner (Perkin-Elmer, Wellesley, MA) at 95% laser power and 85% photomultiplier tube gain. The resulting images were analyzed by ImaGene with signals processed as SN>2.0 (signal to noise ratio).

Statistical analysis

In order to summarize the gene overlap at station and season level, the detected genes from the GeoChip in the three replicates of each station from July and November were deployed as one pool (mean value from the three replicates). The analyses of overlapping genes, unique genes, and diversity indices were performed using an online pipeline (http://ieg.ou.edu/). The proportion of overlapping genes was calculated as the number of overlapping genes divided by the total number of genes detected in both stations. The proportion of unique genes at each station was calculated as the number of unique genes at each station divided by the total number of genes detected at that station.

Statistical analyses of the multi-response permutation procedure (MRPP) and canonical correspondence analysis (CCA) (see below) were performed based on community data from the clone libraries as well as from the GeoChip data. MRPP using Bray-Curtis distance was used to test for significant differences in community composition. The MRPP A-statistics describes the within and between group relatedness relative to what is expected by chance. A p-value <0.05 and an A-statistics >0.1 is considered as significant difference between groups (McCune *et al.*, 2002). To test the relationship between the denitrifier community and the environmental variables, CCA was carried out. The significance of the whole canonical model was tested by 999 permutations. All statistical analyses were carried out in the open source-software R (Team, 2011), using the vegan package (Oksanen, 2011). Stepwise regression was carried out to test the influence of the environmental factors and denitrifier community on potential denitrification rates using SigmaPlot (SigmaPlot, Version 12). Denitrifier communities were converted into univariate variables based on the sample scores for the first two CCA axes.

Results

Physicochemical characteristics

Table 2 lists the seasonal and annual mean values of the physicochemical parameters of the sample sites and the potential denitrification rates in the three mats. The physicochemical parameters fluctuated seasonally and some parameters showed differences between the three mat types. Ammonium concentration was lowest at Station 1 (ST1) and highest at ST3, except in April. Nitrate/nitrite concentrations were in the same range at all stations, albeit with slightly higher concentrations in July and April and slightly lower concentrations in September and January. Phosphate concentration was highest in April and lowest in September at all stations. TOC and TN were similar at ST2 and ST3 but always lowest at ST1.

Potential denitrification rates

$^{29}N_2$ and $^{30}N_2$ were produced at the expected ratio for denitrification given the addition of 99.2-atom% enriched $^{15}NO_3^-$. Denitrification rates (N_2 production) showed remarkable differences between the three stations and varied also seasonally. For ST1 (supratidal, close to the dunes) the potential denitrification rates ranged from 0.1±0.05 - 7.0±1.0 mmol N $m^{-2}d^{-1}$ (Table 2). The denitrification rate was highest in July (7.0±1.0 mmol N $m^{-2}d^{-1}$) and much lower (1.6±0.3 mmol N $m^{-2}d^{-1}$) in September. Denitrification was lowest (0.1±0.05 mmol N $m^{-2}d^{-1}$) in April. The seasonal trend of denitrification at the littoral site (ST3) was slightly different from that at ST1. At ST3, the highest denitrification rate (0.7±0.2 mmol N $m^{-2}d^{-1}$) was in July and was lowest in September (0.1±0.05 mmol N $m^{-2}d^{-1}$). A higher rate (0.5±0.2 mmol N $m^{-2}d^{-1}$) was again observed during January. Unlike the other two sites, the highest rate of denitrification at ST2 (low water mark) (1.6±0.4 mmol N $m^{-2}d^{-1}$) was observed in January and the lowest rate (0.1±0.05 mmol N $m^{-2}d^{-1}$) occurred in July and September. The annual average denitrification rate was highest at the supra-littoral (near the dunes, ST1) (2.8 mmol N $m^{-2}d^{-1}$) and significantly higher ($P<0.05$) than at the other two stations, which were low and not significantly different from each other (0.5 mmol N $m^{-2}d^{-1}$ at ST2 and 0.4 mmol N $m^{-2}d^{-1}$ at ST3).

nirS and *nirK* diversity and composition

nirS and *nirK* sequences from the three stations were analyzed. Combining the clone libraries, 76 unique *nirS* operational taxonomic units (OTUs) and 74 unique *nirK* OTUs (at a 5% distance cut-off) were retrieved. The richness and diversity estimators showed different *nirS* and *nirK* gene richness at the three stations. *nirS*-denitrifier community was richest at ST3, while the other two stations showed a similar richness. *nirK*-denitrifier community was richest at ST1 and poorest at ST3.

Phylogenetic analyses of deduced amino acid sequences for *nirS* and *nirK* gene fragments are shown in Fig. 1. The *nirS* sequences clustered into three distinct groups (Fig. 1A). Group I contained 53%, 36% and 68% of the total sequences from ST1, ST2 and ST3, respectively. The sequences in this group were closely related to the cultivated denitrifier *Marinobacter* sp. U31 (CAF25138) as well as to environmental clones from a hypersaline microbial mat (e.g. CAL69009, CAL69007), an estuarine sediment (e.g. AEK77712, ABY52470) and from the Baltic Sea (e.g. CAJ87449). Group II contained 12%, 64% and 30% sequences from ST1, ST2 and ST3, respectively. Sequences in

Group II clustered closely with those of a variety of cultivated denitrifiers including *Roseobacter denitrificans*, *Paracoccus denitrificans*, and *Silicibacter pomeroyl*. The third group contained 35% and 2% of the sequences of ST1 and ST3. These sequences were closely related to *Pseudomonas stutzeri*, *Azospirillum brasilense* and *Ralstonia eutropha*.

nirK sequences clustered into four groups (Fig. 1B). Group I contained 2%, 81% and 100% of the total *nirK* sequences from ST1, ST2 and ST3, respectively. The sequences belonging to group I were most closely related to environmental clones from San Francisco Bay estuarine sediment (ADM93883) and from the Arabian Sea oxygen minimum zone (ACT98741). Three OTUs from ST1 fell into Group II, showing the best hit of 87% nucleotide sequence similarity with a sequence retrieved from a Chinese agricultural soil (HM628810). Group III contained sequences from ST1 (7%; 17%; 68%, Fig. 1B) and were related to a variety of cultivated denitrifiers, such as *Rhodobacter sphaeroides* (CCA12211) and *Rhodopseudomonas palustris* (NP949481). Group IV comprised only sequences (19%) from ST2. These sequences are closely related to environmental clones from San Francisco Bay estuarine sediment (ADM93844, ADM93870) and remotely related to the cultivated *Alcaligenes* sp. (75% similarity and 48% sequence coverage).

Diversity of *nirS* and *nirK* genes based on GeoChip analysis is summarized in Table 4. A total of 264 *nirS* sequences showed a hybridization signal in at least one of mat. The average number of *nirS* sequences (richness) at ST1 (July), ST2 (July), ST3 (July), ST1 (January), ST2 (January) and ST3 (January) was 253, 206, 146, 215, 161, and 125, respectively (Table 4). Thirty-three sequences were unique and detected only at one of the stations and during one season. In July, ST1 harbored 26 unique sequences, which was 10.3% (26/253) of the total number detected. ST2 and ST3 harbored 2.4% (5/206) and 0.7% (1/146) unique sequences, respectively. In January, the number of unique sequences in ST1 dropped to 3, which was only 1.4% (3/215) of the total number detected. In January no unique sequences were observed at ST2 and ST3. Pairwise comparison of *nirS* sequences showed a high number of overlapping *nirS* sequences between summer and winter as well as between the stations: 81% (ST1 July & January), 72% (ST2 July & January), 70% (ST3 July & January), 74-77% (ST1&ST2), 57% (ST1&ST3) and 68-70% (ST2&ST3).

Similar results were obtained for *nirK* (Table 4). We detected 264 *nirK* sequences in the mats. Most *nirK* sequences were detected in summer at ST1 (256). We detected 204, 141, 214, 150 and 127 *nirK* sequences at ST2 (July), ST3 (July) ST1 (January), ST2 (January) and ST3 (January), respectively (Table 4). In July, ST1 harbored 26 unique sequences, which was 10.2% (26/256) of the total detected sequences. ST2 and ST3 harbored 1.5% (3/204) and 0.7% (1/141) unique sequences of the total detected number, respectively. In January, only 1 unique sequence was detected both at ST1 and ST2. No unique sequence was detected at ST3. Seventy-seven percent of the total detected *nirK* sequences were shared by ST1 and ST2, 54% was shared by ST1 and ST3 and 67% was shared by ST2 and ST3.

The diversity indices for *nirS* and *nirK* were assessed by richness and Shannon-Weaver index (Table 4). At all stations the values for both diversity estimators were higher in summer. The highest richness was observed in summer at ST1 and the lowest value was found in summer and winter at ST3 ($p<0.01$). The highest abundance for both *nirS* and *nirK* were observed in summer at ST1. The lowest abundance for *nirS* was found at ST3 and for *nirK* was found in summer at ST2 and winter at ST3.

Multi-response permutation procedure (MRPP) statistics was carried out to test the differences of the composition of the microbial community between the stations based on *nirS* and *nirK* OTUs obtained from the clone libraries and the GeoChip. MRPP testing of these two data sets gave consistent results. Distinctly different denitrifier communities were found in ST1 when compared to the other two stations ($p<0.05$) from the two data sets. ST2 and ST3 did not contain significantly different communities ($p>0.05$) when the analysis was based on data from the GeoChip but were significantly different when using the data from the clone libraries ($p>0.05$). This was the case for both *nirS* and *nirK* (Table 5). There were no seasonal differences in the denitrifier communities in any of the stations (data not shown). These results were confirmed by CCA analyses (Fig. 2).

Environmental control of denitrifying mat community and activity

No relationship between potential denitrification rates, environmental factors, and the denitrifier community were revealed based on stepwise regression analysis. Canonical correspondence analysis (CCA) was applied in order to discover patterns in the composition of the denitrifying community. Using CCA we analyzed the *nirS* and *nirK* sequence data obtained from the clone libraries and from the GeoChip with the related environmental factors (Table 2).

Figure 2A shows the results of the CCA from the *nirS* sequences obtained from clone libraries. In the diagram, denitrifiers were distinctly grouped according to sample station. There was no effect of the season. The community composition was significantly correlated with all selected variables in the adapted CCA model ($p=0.02$) (based on 999 permutations test). In the CCA diagram (Fig. 2A), the first two axes explained 71% of relationship between the total *nirS* containing community and the environmental factors. The first canonical axis explained 42.5% of total variations ($p=0.008$) and was dominated by the environmental variables TOC ($p<0.05$), TN, and ammonium concentration ($p<0.05$). The second canonical axis explained an additional 28.5% of the constrained variations and was dominated by phosphate ($p<0.05$) and the nitrate+nitrite concentration. The *nirS* containing community in ST1 was distinctly different from those in ST2 and ST3 along the first canonical axis (Axis 1), while the *nirS* containing communities in ST2 and ST3 separated along the second canonical axis (Axis 2). ST2 and ST3 were influenced by both the first and second canonical axes and positively correlated with TOC ($p<0.05$), TN, phosphate ($p<0.05$) and ammonium concentrations ($p<0.05$), but negatively correlated with nitrate+nitrite concentration ($p<0.05$). ST1 was primarily influenced by the first canonical axis, reflecting the role of TOC ($p<0.05$), TN, and ammonium concentrations ($p<0.05$). For each individual variable, a significant correlation was found between community and TOC ($r^2=0.89$, $p=0.003$) and TN ($r^2=0.87$, $p=0.003$), which is indicated by the length of the arrows in the CCA diagram.

Figure 2B shows the CCA profiles based on the seasonal *nirS* community data as obtained from the GeoChip. GeoChip analyses were only performed on the summer and winter samples. Spatially, *nirS* communities from different stations were separated along the first axis of the CCA diagram. Temporally, *nirS* communities of the summer samples were separated from those of the winter samples along the second axis. In general, the community composition was significantly correlated with all selected variables in the adapted CCA model (p=0.001) (based on 999 permutations test). Due to multicollinearity, the C:N ratio, salinity and the potential rate of denitrification were removed. Therefore, five environmental factors were selected and are depicted in the diagram. The first two axes explained 47.7% of the relationship between the total *nirS* community composition and the environment. The first canonical axis explained 33.4% of the total variation (p=0.001). The first axis was dominated by the environmental variables TOC ($p<0.001$), TN ($p<0.001$) and ammonium concentration ($p<0.001$). The second axis explained the rest 14.4% of the total variation ($p =0.001$) and was dominated by phosphate ($p<0.001$) and the nitrate+nitrite concentration ($p< 0.001$). For ST1, the *nirS* community was influenced by all factors taken into account and showed negative correlation with TOC, TN and ammonium concentration. The *nirS* containing community in the summer samples correlated positively with nitrate+nitrite and phosphate concentrations, while the community in the winter samples was negatively correlated with these factors. For ST2, *nirS* in the summer samples was only influenced by the factors reflected by second axis. The *nirS* community in the winter samples was influenced by all the selected factors and was positively correlated with TOC, TN and ammonium concentrations but negatively correlated with phosphate ($p<0.001$) and nitrate+nitrite concentrations. For ST3, the *nirS* community was positively correlated with TOC, TN and ammonium concentrations. The *nirS* in the summer samples also showed a positive correlation with phosphate ($p<0.001$) and nitrate+nitrite concentrations (although this was not significant), while *nirS* in the winter samples was not strongly influenced by any of the environmental variables on the second axis.

Figure 2C and 2D depict the results of the CCA from the *nirK* containing communities. For both the cloning and GeoChip data, the first two axes explained the community composition better than the observations of the *nirS* containing community. The axes 1 and 2 explained 72.1 and 51.7% of the total variation of the *nirK* containing community, respectively. The *nirS and nirK* containing communities responded similarly to spatial and temporal variation of the environmental factors.

Discussion

The few existing studies on denitrification in microbial mats used the acetylene inhibition technique (AI). The published rates of denitrification in microbial mats ranged from 0 to 3.14 mmol N m^{-2} d^{-1} (Bonin & Michotey, 2006; Desnues *et al.*, 2007; Joye & Paerl, 1994). In the present study, we measured potential denitrification rates by the isotope pairing (IP) technique using small cores of the mat from 0.06 to 7.00 mmol N m^{-2} d^{-1} and, hence, were in the same range. We do realize that such comparisons fall short because of differences that are inherent of the technique as well as different incubations (i.e. intact cores *versus* slurries). E.g. Lohse *et al*. (1996) concluded that the AI technique underestimated the rate of denitrification by a factor of two when compared to the IP technique. Also Bonin & Michotey (2006) measured denitrification in a microbial mat in the Camargue using both the AI and IP techniques and found that the latter gave 10-fold higher rates. However, the AI technique is not adequate when denitrification depends on nitrification in the sediment, because acetylene blocks the latter. Our measurements did not depend on nitrification since we added ample nitrate.

A previous study on the same mats revealed that in summer nitrogen fixation was 2.0, 0.5 and 2.1 mmol N m^{-2} d^{-1} for the stations 1, 2 and 3, respectively (Severin & Stal, 2008). Similar mats on the German Wadden Sea barrier island Mellum fixed 3.2, 0.2 and 1.0 mmol N m^{-2} d^{-1} for the stations that were representative for those studied here (station 1, 2 and 3, respectively) (Stal *et al.*, 1984). Hence, these values indicate that denitrification and N_2 fixation are in the same range in the coastal mats studied here. Joye & Paerl (1994) measured denitrification by the AI technique and showed that denitrification was only 15% of N_2 fixation on an annual basis in the mats of Tomales Bay. However, given that denitrification is underestimated by the AI technique, denitrification may have been responsible for a much higher proportion of the loss of the fixed N_2. Also, Bonin & Michotey (2006) found that denitrification exceeded N_2 fixation in winter in the hypersaline mat in Camargue. Hence, we conclude that denitrification can be an important sink for the fixed nitrogen in microbial mats.

Spatial and temporal heterogeneity of potential denitrification rates were observed in the present study and have also been documented for other microbial mats (Bonin & Michotey, 2006; Joye & Paerl, 1994). ST1 and ST3 showed the highest potential denitrification rates in summer (July), which was consistent with what has been reported for the hypersaline mats in the Camargue (Bonin & Michotey, 2006) and for the mudflat mats in Tomales Bay (Joye & Paerl, 1994). These results suggest that the nitrogen cycle in different phototrophic microbial mats behaves in a similar way. This might be due to the fact that microbial processes in phototrophic microbial mats are fundamentally the same and driven by the physicochemical gradients typically existing in these ecosystems (Stal, 2012).

The potential rate of denitrification in each of the mats can most likely be attributed to the dissimilar denitrifier communities. Denitrifiers are phylogenetically diverse and therefore it is expected that the physiology and enzyme affinities may vary considerably (Philippot & Hallin, 2005). Consequently, shifts in community composition would lead to changes in the potential rate of denitrification and this has actually been shown in several cases (Cavigelli&Robertson, 2000; Jayakumar et al., 2004; Rich et al., 2003).

We used GeoChip and clone libraries to investigate the denitrifier community in microbial mats. Clone libraries offer the possibility to discover novel species of denitrifiers (assessed by evaluating and analyzing the *nirS* and *nirK* genes) in the microbial mats. However, the limited numbers of clones that were sequenced and the bias of the PCR approach targeting mainly dominant groups could have underestimated the rare types. Therefore we used in addition the GeoChip. This chip provides a high coverage of the *nirS* and *nirK* genes that are not sufficient abundant to be retrieved by clone libraries, provided that their probes were included on the chip. The combination of these two approaches allowed us to obtain a comprehensive diversity of the *nirS*- and *nirK*-denitrifiers in the microbial mats. The results from both analyses were in agreement with each other.

The phylogenetic analysis of the denitrifier community using *nirS* and *nirK* revealed that denitrifiers inhabited all three types of microbial mats. Most of the *nirS* and *nirK* genes retrieved in this study were unrelated to known denitrifying bacteria but shared considerable phylogenetic similarity with sequences from diverse environments including estuarine (Santoro *et al.*, 2006), marine habitats (Castro-Gonzalez *et al.*, 2005) as well as soil (Throbäck *et al.*, 2007) and sludge (Osaka *et al.*, 2006). This suggests that a large number of the denitrifiers in these microbial mats have not yet been cultivated. The high diversity of the denitrifier community may be due to a variety of potential environmental niches present in the microbial mats, which would allow diverse denitrifiers to proliferate. The deduced amino acid sequences of *nirS* and *nirK* fragments retrieved from clone libraries made from each of the sample stations were more similar to each other than to those of the other stations and hardly overlapped with the sequences from other stations. Although the *nirS* phylogenetic tree did not show a clear division of the clones according to the stations from which they originated, as was the case for the *nirK* tree, CCA analyses confirmed that both *nirS*- and *nirK*-denitrifier communities partitioned according to the different mat types. This shows that the conditions that prevail in a certain mat type selects for the type of denitrifier. This is in agreement with a clone library based study of a denitrifier community along a salinity and nitrate gradient in a coastal aquifer. Santoro and coworkers found that both NirS and NirK were distinct for certain communities, exhibiting little overlap between stations (Santoro *et al.*, 2006). This habitat specificity of *nirS*- and *nirK*- denitrifier communities was observed in various other environments such as the Baltic Sea and freshwater lakes (Kim *et al.*, 2011) or soils (Prieme *et al.*, 2002).

Diversity estimates (Shannon-Weaver) based on the clone library GeoChip indicated that ST1 harbored a more diverse *nirK*-type denitrifying community than the other two stations. With respect to *nirS* diversity, estimates made by clone libraries and the GeoChip were not consistent and we are therefore unable to draw a conclusion for this gene. The stringency of hybridization was optimized (Wu *et al*., 2006). The group-specific probes matched perfectly with their targets and the false positive signal was negligible. Most unique *nirS* and *nirK* were detected at ST1 suggesting that this station is different from the other two. Moreover, the phylogenetic trees of translated *nirS* and *nirK* from ST2 and ST3 show that a large number of sequences fell into the same clusters, suggesting that the denitrifying communities of these two stations were similar. The *nirS* and *nirK* sequences from ST1 formed distinct clusters. Multi-response permutation procedure analysis based on clone libraries and GeoChip of *nirS* and *nirK* confirmed that the similarity was higher between ST2 and ST3 than either of these stations to ST1. Hence, in this respect the dissimilarity of the denitrifying communities in the three stations did not follow the pattern of the whole microbial community (Bolhuis & Stal, 2011). These authors found that the microbial community of ST2 was more dissimilar from that of ST1 and ST3. The *nirS*- and *nirK* denitrifiers showed higher diversity during summer and a lower diversity during winter. This is in agreement with the development of a mat, which grows to maturity during summer and growth stops during winter when the mat is degraded (Stal *et al.*, 1985).

The spatial organization of the denitrifying community in the microbial mats was likely the result of the different environmental conditions. Salinity has been proposed as the major driver of the microbial community composition for these microbial mats (Bolhuis *et al.*, 2013). This might also apply to the denitrifier community. Jones & Hallin (2010) concluded that the global distribution pattern of *nirS* and *nirK* genes corresponded to salinity. The lower salinity at ST1 may explain the higher diversity of the denitrifier community. This has also been observed in a benthic denitrifier community along the estuarine gradient in Chesapeake Bay (Bulow *et al.*, 2008). These authors found the highest *nirS* diversity at a freshwater station and the lowest diversity at a station with high salinity. Nitrite reductase genes in a wastewater treatment system showed that salinity decreased the diversity of both *nirS* and *nirK* containing denitrifying bacteria (Yoshie *et al.*, 2004). Similar observations have been made for other functional genes of the N-cycle. Severin *et al.* (2012) investigated the same mats as in this study and found that the proportion of cyanobacterial *nifH* transcripts decreased with increasing salinity. Likewise, Bernhard *et al*. (2010) found that the loss of diversity of ammonia-oxidizing bacteria correlated with increasing salinity in the Plum Island Sound estuary. Possible factors for the denitrifier compositional changes were partly associated with but not exclusively driven by salinity.

Canonical correspondence analysis of the *nirS* and *nirK* genes indicated that organic substrates and nitrate/nitrite are also important environmental factors influencing the denitrifier community composition but in opposite ways. Nitrite is the electron acceptor in denitrification. The nitrate/nitrite concentration at ST1 was slightly higher than at the other two stations and this might be the underlying reason for the different denitrifier community in this station (Table 2). This is in line with the observation of Liu *et al.* (2003) who found that denitrifying communities were similar when the nitrate concentrations were at the same level. Organic carbon is the primary electron donor for heterotrophic denitrifiers (Zumft, 1997). We showed that the highest diversity of the denitrifier community was at the station with the lowest concentration of organic matter (Table 2). Most of this organic matter is recalcitrant polymeric material (Stal, 2003). We conceive that this would increase the diversity of denitrifiers. When organic matter is available, diversity will be low because of strong competition and out-competing of the less adapted species.

The two dimensions of CCA explained only part of the total variance of the denitrifier community (Fig. 2). This implies that there are also other factors that contribute to the composition of microbial community. For example, interaction and competition for resources with other microorganisms could be additional factors. In the microbial mats, denitrifiers compete for nitrate+nitrite with the primary producers such as cyanobacteria and diatoms that represent dominant groups in these mats (Bolhuis & Stal, 2011; Severin *et al.*, 2010). The diversity of the *nifH* gene in these mats varied in a similar way (Severin & Stal, 2010). These authors found that the diazotrophic communities of ST2 and 3 were more similar to each other than to ST1. These results suggest that regardless different functional genes (*nifH*, *nirS* and *nirK*), the structure of the mats and its position in the littoral gradient overwhelmingly drive the diversity of the community, rather than single geochemical factors.

NirS and NirK nitrite reductases are functionally equivalent, but there is a debate going on as to whether the two types of denitrifiers are ecologically distinct (Jones & Hallin, 2010). Smith & Ogram (2008) found that *nirS*- and *nirK*- denitrifiers responded differently to environmental gradients. In this study, we found that *nirS*- and *nirK*- denitrifiers were similarly affected by environmental variables (Fig. 2). However, although this does not exclude the possibility that the two types of denitrifiers inhabit different niches, we have also no evidence for the opposite that they occupy the same niche. Desnues *et al.* (2007) investigated the vertical zonation of *nirS*- and *nirK*- denitrifiers in a hypersaline mat. These authors found that *nirS* was mainly localized in the permanent anoxic layer whereas *nirK* occurred throughout the whole mat and seemed to be better adapted to environmental fluctuations. Shannon index based on *nirS* and *nirK* sequences indicated a higher diversity of *nirS* clones compared to *nirK* clones at station 3. This finding agrees with observations from another ecosystem (Mosier & Francis, 2010). However, the opposite was found for the stations 1 and 2. The seasonal changes of abundance of *nirS* and *nirK* were not consistent and varied between stations. This would imply that *nirS*- and *nirK*-denitrifiers adapt differently to the environment. As illustrated in a previous study (Santoro *et al.*, 2006), caution is needed because comparisons by using richness estimates may vary according to sample size. The GeoChip results showed a similar diversity and richness for *nirS* and *nirK*. It has been shown that in some ecosystems *nirS*-denitrifiers were more abundant than *nirK*-denitrifiers (Mosier & Francis, 2010). In our study, *nirS*- and *nirK*-denitrifiers were equally abundant in the GeoChip analysis, suggesting that both types of denitrifiers play important roles in denitrification in the microbial mats.

References:

Bernhard AE, Landry ZC, Blevins A, de la Torre JR, Giblin AE & Stahl DA (2010) Abundance of ammonia-oxidizing archaea and bacteria along an estuarine salinity gradient in relation to potential nitrification rates. *Appl Environ Microbiol* **76:** 1285-1289.

Bolhuis H & Stal LJ (2011) Analysis of bacterial and archaeal diversity in coastal microbial mats using massive parallel 16S rRNA gene tag sequencing. *ISME J* **5:** 1701-1712.

Bolhuis H, Fillinger L & Stal LJ (2013) Coastal microbial mat diversity along a natural salinity gradient. *PLoS ONE* **8(5):** e63166.

Bonin PC & Michotey VD (2006) Nitrogen budget in a microbial mat in the Camargue (southern France). *Mar Ecol Prog Ser* **322:** 75-84.

Braker G, Zhou JZ, Wu LY, Devol AH & Tiedje JM (2000) Nitrite reductase genes (*nirK* and *nirS*) as functional markers to investigate diversity of denitrifying bacteria in Pacific northwest marine sediment communities. *Appl Environ Microbiol* **66:** 2096-2104.

Bulow SE, Francis CA, Jackson GA & Ward BB (2008) Sediment denitrifier community composition and nirS gene expression investigated with functional gene microarrays. *Environ Microbiol* **10:** 3057-3069.

Castro-Gonzalez M, Braker G, Farias L & Ulloa O (2005) Communities of *nirS*-type denitrifiers in the water column of the oxygen minimum zone in the eastern South Pacific. *Environ Microbiol* **7:** 1298-1306.

Cavigelli MA&Robertson GP (2000) The functional significance of denitrifier community composition in a terrestrial ecosystem. *Ecology* **81:** 1402-1414.

Desnues C, Michotey VD, Wieland A, Zhizang C, Fourcans A, Duran R & Bonin PC (2007) Seasonal and diel distributions of denitrifying and bacterial communities in a hypersaline microbial mat (Camargue, France). *Water Res* **41:** 3407-3419.

Hallin S, Jones CM, Schloter M & Philippot L (2009) Relationship between N-cycling communities and ecosystem functioning in a 50-year-old fertilization experiment. *ISME J* **3:** 597-605.

Hannig M, Braker G, Dippner J & Jürgens K (2006) Linking denitrifier community structure and prevalent biogeochemical parameters in the pelagial of the central Baltic Proper (Baltic Sea). *FEMS Microbiol Ecol* **57:** 260-271.

He ZL, Deng Y, Van Nostrand JD *et al.* (2010) GeoChip 3.0 as a high-throughput tool for analyzing microbial community composition, structure and functional activity. *ISME J* **4:** 1167-1179.

Jayakumar DA, Francis CA, Naqvi SWA & Ward BB (2004) Diversity of nitrite reductase genes (*nirS*) in the denitrifying water column of the coastal Arabian Sea. *Aquat Microb Ecol* **34:** 69-78.

Jones CM & Hallin S (2010) Ecological and evolutionary factors underlying global and local assembly of denitrifier communities. *ISME J* **4:** 633-641.

Joye SB & Paerl HW (1994) Nitrogen cycling in microbial mats: rates and patterns of denitrification and nitrogen fixation. *Mar Biol* **119:** 285-295.

Kim O-S, Imhoff J, Witzel K-P & Junier P (2011) Distribution of denitrifying bacterial communities in the stratified water column and sediment–water interface in two freshwater lakes and the Baltic Sea. *Aquat Ecol* **45:** 99-112.

Liang YT, He ZL, Wu LY, Deng Y, Li GH & Zhou JZ (2010) Development of a Common oligonucleotide reference standard for microarray data normalization and comparison across different microbial communities. *Appl Environ Microbiol* **76:** 1088-1094.

Liu XD, Tiquia SM, Holguin G, Wu LY, Nold SC, Devol AH, Luo K, Palumbo AV, Tiedje JM & Zhou JZ (2003) Molecular diversity of denitrifying genes in continental margin sediments within the oxygen-deficient zone off the Pacific coast of Mexico. *Appl Environ Microbiol* **69:** 3549-3560.

Lohse L, Kloosterhuis HT, vanRaaphorst W & Helder W (1996) Denitrification rates as measured by the isotope pairing method and by the acetylene inhibition technique in continental shelf sediments of the North Sea. *Mar Ecol Prog Ser* **132:** 169-179.

McCune B, Grace JB & Urban DL (2002) Analysis of ecological communities, vol. 28. MjM Software Design Gleneden Beach, Oregon.

Mosier AC & Francis CA (2010) Denitrifier abundance and activity across the San Francisco Bay estuary. *Environ Microbiol Rep* **2:** 667-676.

Oakley BB, Francis CA, Roberts KJ, Fuchsman CA, Srinivasan S & Staley JT (2007) Analysis of nitrite reductase (*nirK* and *nirS*) genes and cultivation reveal depauperate community of denitrifying bacteria in the Black Sea suboxic zone. *Environ Microbiol* **9:** 118-130.

Oksanen J (2011) Multivariate analysis of ecological communities in R: vegan tutorial. *R package version*: 2.0-1.

Osaka T, Yoshie S, Tsuneda S, Hirata A, Iwami N & Inamori Y (2006) Identification of acetate- or methanol-assimilating bacteria under nitrate-reducing conditions by stable-isotope probing. *Microb Ecol* **52:** 253-266.

Philippot L & Hallin S (2005) Finding the missing link between diversity and activity using denitrifying bacteria as a model functional community. *Curr Opinion Microbiol* **8:** 234-239.

Prieme A, Braker G & Tiedje JM (2002) Diversity of nitrite reductase (*nirK* and *nirS*) gene fragments in forested upland and wetland soils. *Appl Environ Microbiol* **68:** 1893-1900.

Rich JJ, Heichen RS, Bottomley PJ, Cromack K&Myrold DD (2003) Community composition and functioning of denitrifying bacteria from adjacent meadow and forest soils. *Appl Environ Microbiol* **69:** 5974-5982.

Santoro AE, Boehm AB & Francis CA (2006) Denitrifier community composition along a nitrate and salinity gradient in a coastal aquifer. *Appl Environ Microbiol* **72:** 2102-2109.

Severin I & Stal LJ (2008) Light dependency of nitrogen fixation in a coastal cyanobacterial mat. *ISME J* **2:** 1077-1088.

Severin I, Acinas SG & Stal LJ (2010) Diversity of nitrogen-fixing bacteria in cyanobacterial mats. *FEMS Microbiol Ecol* **73:** 514-525.

Severin I & Stal LJ (2010) Spatial and temporal variability in nitrogenase activity and diazotrophic community composition in coastal microbial mats. *Mar Ecol Prog Ser* 417:13-25

Severin I, Confurius-Guns V & Stal LJ (2012) Effect of salinity on nitrogenase activity and composition of the active diazotrophic community in intertidal microbial mats. *Arch Microbiol* **194:** 483-491.

Smith JM & Ogram A (2008) Genetic and functional variation in denitrifier populations along a short-term restoration chronosequence. *Appl Environ Microbiol* **74:** 5615-5620.

Stal LJ, Grossberger S & Krumbein WE (1984) Nitrogen fixation associated with the cyanobacterial mat of a marine laminated microbial ecosystem. *Mar Biol* **82:** 217-224.

Stal LJ, Van Gemerden H & Krumbein WE (1985) Structure and development of a benthic marine microbial mat. *FEMS Microbiol Ecol* **31:** 111-125.

Stal LJ (2001) Coastal microbial mats: the physiology of a small-scale ecosystem. *S Afr J Bot* **67:** 399-410.

Stal LJ (2003) Nitrogen cycling in marine cyanobacterial mats. In: Krumbein WE, Paterson DM, Zavarzin GA (eds). *Fossil and Recent biofilms: a natural history of life on Earth*. Springer. pp 119-140.

Stal LJ (2012) Microbial mats and stromatolites. In: Whitton BA (ed). *Ecology of Cyanobacteria II: Their Diversity in Space and Time*, Springer, Dordrecht. pp 65-125.

Team RDC (2011) R: A language and environment for statistical computing. Vienna, Austria: R Foundation for Statistical Computing; 2008. ISBN 3-900051-07–0. Available at: http://www. R-project. org.

Thamdrup B & Dalsgaard T (2002) Production of N_2 through anaerobic ammonium oxidation coupled to nitrate reduction in marine sediments. *Appl Environ Microbiol* **68:** 1312-1318.

Throbäck IN, Enwall K, Jarvis Å & Hallin S (2004) Reassessing PCR primers targeting *nirS*, *nirK* and *nosZ* genes for community surveys of denitrifying bacteria with DGGE. *FEMS Microbiol Ecol* **49:** 401-417.

Throbäck IN, Johansson M, Rosenquist M, Pell M, Hansson M & Hallin S (2007) Silver (Ag^+) reduces denitrification and induces enrichment of novel *nirK* genotypes in soil. *FEMS Microbiol Lett* **270:** 189-194.

Wu LY, Liu X, Schadt CW & Zhou JZ (2006) Microarray-based analysis of subnanogram quantities of microbial community DNAs by using whole-community genome amplification. *Appl Environ Microbiol* **72:** 4931-4941.

Yoshie S, Noda N, Tsuneda S, Hirata A & Inamori Y (2004) Salinity decreases nitrite reductase gene diversity in denitrifying bacteria of wastewater treatment systems. *Appl Environ Microbiol* **70:** 3152-3157.

Zumft W (1997) Cell biology and molecular basis of denitrification. *Microbiol Mol Biol Rev* **61:** 533-616.

Acknowledgments

This work was financially supported by the Dutch Organization for Scientific Research, Earth and Life Science (NWO-ALW) grant 839.08.332. The authors are indebted to Dr. Jizhong (Joe) Zhou and his team at the University of Oklahoma for hosting HF to carry out the GeoChip analyses. We also thank Veronique Confurius and Dr. Juliette Ly for their help with the fieldwork.

Tables:

Table 1. The geographical coordinates and description of the mats investigated in this study.

Station	Geographical coordinates	Description
Station 1 (ST1)	53°29.445′N, 6°8.718′E	Mainly freshwater influenced site, close to the dunes. Irregularly inundated.
Station 2 (ST2)	53°29.460′N, 6°8.309′E	Seawater influenced site, developing microbial mat. At the low water mark.
Station 3 (ST3)	53°29.445′N, 6°8.342′E	Seawater and freshwater influenced site, located between ST1 and ST2, at the edge of the salt marsh

Table 2. Physicochemical parameters and potential denitrification rates in the microbial mats during the 2010 sampling period.

	July (2010)	September (2010)	January (2010)	April (2011)
Station 1				
Temperature (°C, sediment)	17	10	0	8
NH_4^+ (μmol/l)	128.9±3.0	83.7±17.3	191.3±23.4	233.1±23.7
NO_X^- (μmol/l)	23.3±4.6	8.4±1.1	9.6±4.6	25.9±3.4
PO_4^{3-} (μmol/l)	20.1±6.1	3.1±0.5	n.d.	25±3.8
TOC (%)	0.04	0.06	0.04	0.04
TN (%)	0.006	0.01	0.007	0.007
C/N	6.7	6.0	5.7	5.7
Salinity (psu)	18	19	15	17
Denitrification (mmol N $m^{-2}d^{-1}$)	7.0±1.0	1.6±0.3	2.4±0.3	0.1±0.05
Station 2				
Temperature (°C, sediment)	17	10	0	8
NH_4^+ (μmol/l)	587.9±41.2	216.2±69.8	736.8±199.6	486.1±61.3
NO_X^- (μmol/l)	22.4±14.7	8.7±1.4	6.2±1.1	20.6±4.5
PO_4^{3-} (μmol/l)	19.7±2.0	3.2±0.9	n.d.	58.6±26.3
TOC (%)	0.19±0.01	0.20±0.03	0.20±0.03	0.17±0.02
TN (%)	0.03	0.04	0.03	0.03
C/N	6.3	5.0	6.7	5.7
Salinity (psu)	28	28	30	28
Denitrification (mmol N $m^{-2}d^{-1}$)	0.1±0.05	0.1±0.05	1.6±0.4	0.2±0.1
Station 3				
Temperature (°C, sediment)	17	10	0	8
NH_4^+ (μmol/l)	217.3±102.3	255.9±68.4	510.2±62.2	475.8±3.5
NO_X^- (μmol/l)	16.0±3.7	7.6±1.9	2.8±0.6	19.6±4.0
PO_4^{3-} (μmol/l)	28.5±15.2	3.9±1.2	n.d.	48.5±10.6
TOC (%)	0.11±0.03	0.15±0.02	0.15±0.02	0.13±0.02
TN (%)	0.02	0.03	0.03	0.02
C/N	5.5	5.0	5.0	6.5
Salinity (psu)	25	25	22	23
Denitrification (mmol N $m^{-2}d^{-1}$)	0.7±0.2	0.1±0.05	0.5±0.2	0.1±0.05

Abbreviations: n.d., no data; TOC, total organic carbon; TN, Total nitrogen.

Table 3. Richness and diversity statistics of *nirS* and *nirK* clone libraries based on 95% cutoffs.

	No. of clones	No. of OTUs	ACE	Chao1	Shannon	Simpson
nirS						
ST1	55	20	56	42	2.1	0.25
ST2	48	19	131	49	2.2	0.18
ST3	66	32	48	47	3.2	0.03
nirK						
ST1	70	35	481	194	3.3	0.05
ST2	69	27	122	84	2.6	0.18
ST3	52	17	41	30	2.1	0.13

Table 4. Summary of *nirS* and *nirK* genes detected by GeoChip, including the number and percentage of overlapping (italic) and unique (bold) sequences, the diversity indices and abundance for each station.

	ST1_July	ST2_July	ST3_July	ST1_Jan.	ST2_Jan.	ST3_Jan.
nirS						
ST1_July	**26(10.3%)**	*200(77.2%)*	*144(56.5%)*	*210(81.4%)*	*159(62.4%)*	*124(48.8%)*
ST2_July		**3(1.5%)**	*145(70.1%)*	*185(78.4%)*	*154(72.3%)*	*123(59.1%)*
ST3_July			**1(0.7%)**	*139(62.6%)*	*123(66.9%)*	*112(70.4%)*
ST1_Jan.				**3(1.4%)**	*161(74.9%)*	*124(57.4%)*
ST2_Jan.					**0(0.00%)**	*116(68.2%)*
ST3_Jan.						**0(0.00%)**
Richness*	253	206	146	215	161	125
Shannon-Weaver (H)	5.5	5.3	5	5.4	5.1	4.8
Abundance (%)**	8.2	7.7	7.4	7.9	7.8	7.4
nirK						
ST1_July	**26(10.2%)**	*200(76.9%)*	*139(53.9%)*	*212(82.2%)*	*147(56.8%)*	*124(47.9%)*
ST2_July		**1(0.5%)**	*139(67.5%)*	*184(78.6%)*	*144(68.6%)*	*126(61.5%)*
ST3_July			**1(0.7%)**	*134(60.6%)*	*117(67.2%)*	*116(76.3%)*
ST1_Jan.				**1(0.5%)**	*145(66.2%)*	*122(55.7%)*
ST2_Jan.					**1(0.7%)**	*116(72.1%)*
ST3_Jan.						**0(0.00%)**
Richness *	256	204	141	214	150	127
Shannon-Weaver (H)	5.5	5.3	4.9	5.4	5	4.8
Abundance (%)**	8.3	7.6	7.3	7.9	7.3	7.6

* richness was determined as probe numbers detected.

**abundance was determined by dividing the hybridization intensity of *nirS* or *nirK* on the GeoChip by the total signal of all nitrogen cycling genes detected on the array.

Table 5. MRPP A-vales of the denitrifier community composition.

Difference between group		
Spatial differences	A-value (clone library)	A-value (GeoChip)
nirS		
ST1 vs ST2	0.753 (p=0.024)*	0.190 (p=0.002)*
ST1 vs ST3	0.749 (p=0.018)*	0.400 (p=0.001)*
ST2 vs ST3	0.667 (p=0.027)*	0.059 (p=0.108)
nirK		
ST1 vs ST2	0.604 (p=0.029)*	0.242 (p=0.004)*
ST1 vs ST3	0.721 (p=0.045)*	0.454 (p=0.002)*
ST2 vs ST3	0.501 (p=0.020)*	0.66 (p=0.096)

* means p<0.05 (statistical difference between whole *nirS* and *nirK* profiles assessed using multi-response permutation procedure).

Legends

Figure 1. Phylogenetic trees for *nirS* (A) and *nirK* (B) genes, based on the translated amino acid sequence, constructing by neighbor-joining method in MEGA 5. Sequences from this study were shown as the percentage of environmental clones from each station. Significant bootstrap values (>50) are shown at branch nodes.

Figure 2. Canonical correspondence analysis of the denitrifier community composition of mat samples. (A) and (C): analysis based on *nirS* and *nirK* clone data and points represent the denitrifier community from seasonal samples at indicated station. (B) and (D): analysis based on *nirS* and *nirK* GeoChip data and points represent replicated denitrifier community from summer and winter samples at indicated station (S: summer; W: winter). Arrows represent the relationship between environmental parameters with the denitrifier communities.

Figures:

Fig. 1

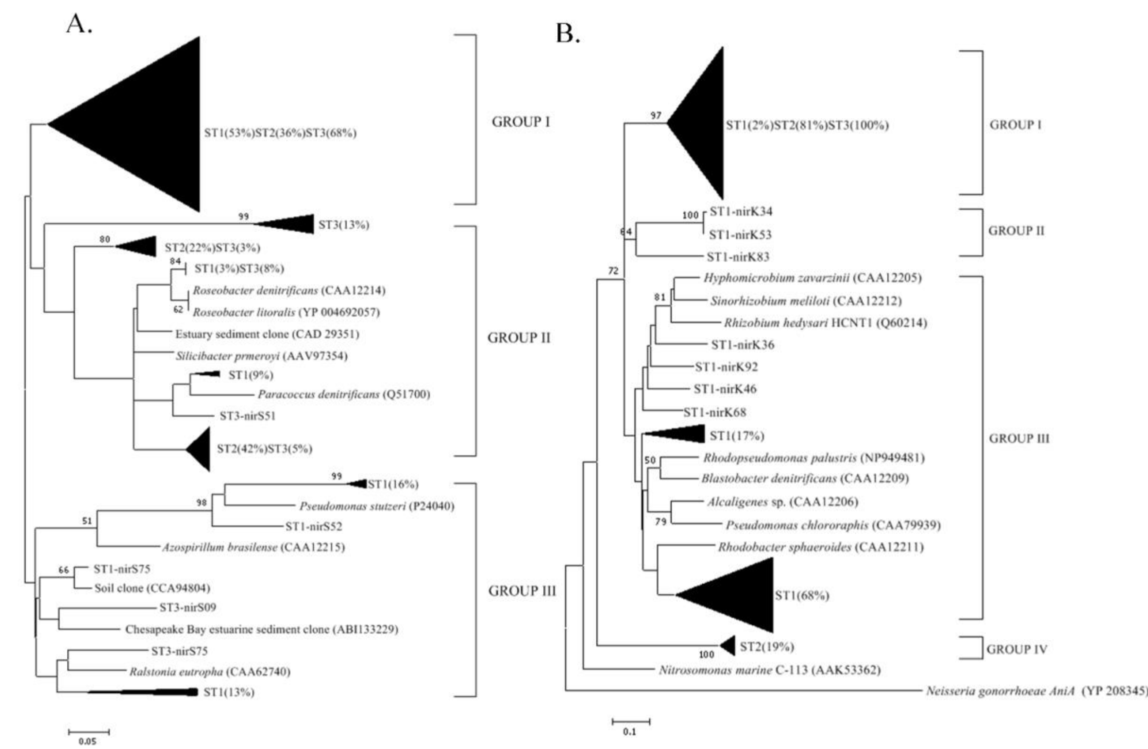

Fig. 2

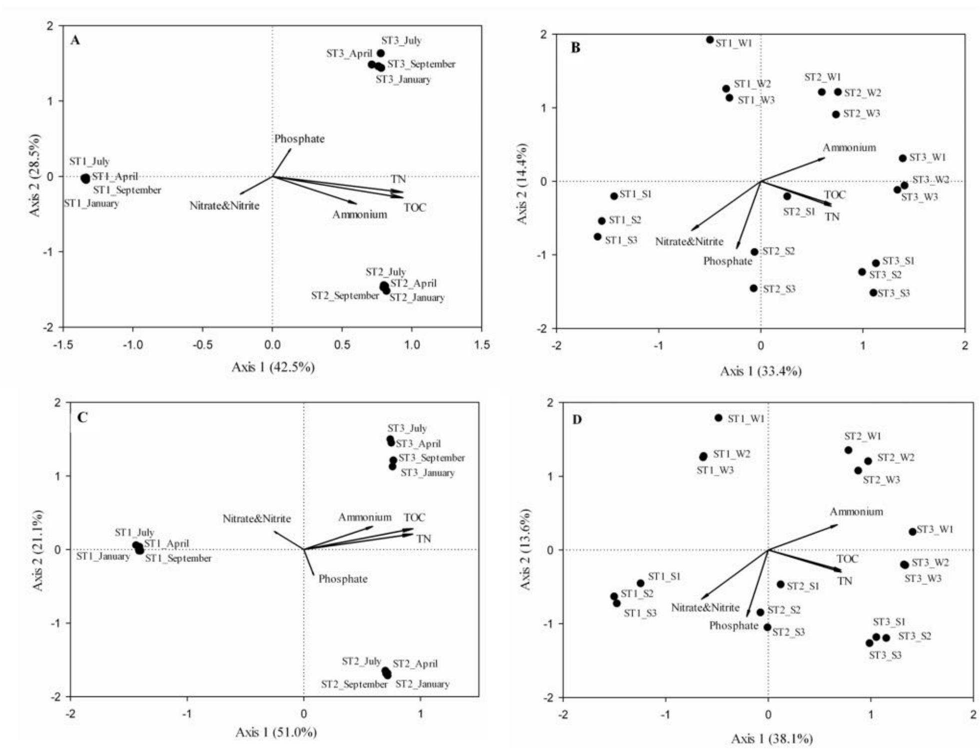
A
ST3_July
ST3_April
ST3_September
ST3_January
Phosphate
ST1_July
ST1_April
ST1_September
ST1_January
Nitrate&Nitrite
TN
TOC
Ammonium
ST2_July
ST2_April
ST2_September
ST2_January
Axis 1 (42.5%)
Axis 2 (28.5%)
B
ST1_W1
ST1_W2
ST1_W3
ST2_W1
ST2_W2
ST2_W3
Ammonium
ST3_W1
ST3_W2
ST3_W3
ST1_S1
ST1_S2
ST1_S3
TOC
TN
ST2_S1
Nitrate&Nitrite
Phosphate
ST2_S2
ST2_S3
ST3_S1
ST3_S2
ST3_S3
Axis 1 (33.4%)
Axis 2 (14.4%)
C
ST3_July
ST3_April
ST3_September
ST3_January
Nitrate&Nitrite
Ammonium
TOC
TN
ST1_July
ST1_April
ST1_January
ST1_September
Phosphate
ST2_July
ST2_April
ST2_September
ST2_January
Axis 1 (51.0%)
Axis 2 (21.1%)
D
ST1_W1
ST1_W2
ST1_W3
ST2_W1
ST2_W2
ST2_W3
Ammonium
ST3_W1
TOC
TN
ST3_W2
ST3_W3
ST1_S1
ST1_S2
ST1_S3
ST2_S1
Nitrate&Nitrite
ST2_S2
Phosphate
ST2_S3
ST3_S1
ST3_S2
ST3_S3
Axis 1 (38.1%)
Axis 2 (13.6%)